Theor Chim Acta (1986) 70: 189-202

Theoretica Chimica Acta

Theoretical interpretation of Mössbauer spectra of ^{119}Sn compounds

V. Männing[1] and M. Grodzicki[2]

[1] Institut für Physikalische Chemie, Universität Hamburg, Laufgraben 24, D-2000 Hamburg 13, Federal Republic of Germany

[2] I. Institut für Theoretische Physik, Universität Hamburg, Jungiusstr. 9, D-2000 Hamburg 36, Federal Republic of Germany

(Received June 28, 1985, revised June 20/Accepted June 23, 1986)

Experimental Mössbauer spectra of a series of Sn(II) and Sn(IV) compounds are interpreted in terms of MO theory. On the basis of the self-consistent charge (SCC)-Xα-MO method electronic charge densities $\rho(0)$ and electric field gradients V_{zz} at the ^{119}Sn nucleus are computed and related with experimental isomer shifts δ and quadrupole splittings ΔE_q. From this correlation values for the fractional change $\delta R/R$ in the nuclear charge radius and for the nuclear quadrupole moment Q of ^{119}Sn are obtained as $\delta R/R = 1.61 \cdot 10^{-4}$ and $Q = -0.0615b$, respectively. The results of our MO calculations indicate that large isomer shift differences in ^{119}Sn compounds are due to a "lone-pair" MO, which exists in Sn(II) compounds but is absent in Sn(IV) compounds. This "lone-pair" MO causes an increase mainly in the 5s orbital population, resulting in a large electronic charge density $\rho(0)$. Furthermore, our results show the limits of the applicability of simple electrostatic models or phenomenological schemes to the interpretation of the experimental data when different coordination numbers of Sn are involved.

Key words: Mössbauer spectroscopy — Tin compounds

1. Introduction

The purpose of our work is to demonstrate the necessity of applying molecular orbital (MO) calculations to understand experimental Mössbauer spectra in terms of electronic structure data. Since the results of our MO calculations indicate

that, in general, unequivocal informations about the electronic structure of molecules cannot be obtained from Mössbauer spectra alone, Mössbauer data have to be supplemented either by additional experimental studies (e.g. ESR or NMR measurements) or by theoretical calculations. On the other hand, although sufficiently accurate MO calculations based on many-electron approaches (e.g. CI or Green's functions calculations) yield in principle all desired information about the electronic structure to any degree of reliability, such calculations are almost impossible for larger molecules containing heavy atoms. Therefore, a practical way of gaining insight into the bonding properties and electronic structure of such systems consists of combining semiempirical MO calculations with experimental data to derive reliable informations. Up to now semiempirical MO calculations on ^{119}Sn compounds are few in number and of uncertain reliability. We mention, however, the encouraging attempt of Winkler and Mehner [1] to apply Hückel methods to the interpretation of isomer shift data for Sn(IV) compounds.

2. Molecular orbital calculations

The SCC-Xα method [2] treating only valence electrons explicitly is based on the secular equation

$$\sum_{\nu j} (H_{ij}^{\mu\nu} - \varepsilon_k S_{ij}^{\mu\nu}) c_{jk}^{\nu} = 0 \tag{1}$$

where ε_k are the molecular orbital energies, $S_{ij}^{\mu\nu}$ are overlap matrix elements, c_{jk}^{ν} are the LCAO coefficients, and the indices μ, ν number the atoms, while i, j denote the atomic wave functions centered on the μth and νth atom, respectively. The matrix elements $H_{ij}^{\mu\nu}$ of the Hamiltonian are given as [2]

$$H_{ij}^{\mu\nu} = \tfrac{1}{2}(\varepsilon_i^{\mu} + \varepsilon_j^{\nu}) S_{ij}^{\mu\nu} + \tfrac{1}{2}(V_{ij}^{\mu\nu} + V_{ji}^{\nu\mu}). \tag{2}$$

Here the valence orbital ionization potential ε_j^{ν} and the matrix elements $V_{ij}^{\mu\nu}$ of the molecular potential depend on the effective atomic charge

$$Q_{\nu} = Z_{\nu} - N_{\nu} \tag{3}$$

where Z_{ν} is the nuclear charge and N_{ν} is the number of electrons. Thus, the self-consistent cycle has the following structure:

$$\{Q_{\nu}\}_{\text{initial}} \rightarrow H_{ij}^{\mu\nu}(\{Q_{\nu}\}) \rightarrow \varepsilon_k, \psi_k(\vec{r}) \rightarrow P_{ij}^{\mu\nu} \rightarrow \{Q_{\nu}\}_{\text{new}} \tag{4}$$

with the bond-order matrix $P_{ij}^{\mu\nu}$ given by

$$P_{ij}^{\mu\nu} = \sum_k n_k c_{ik}^{\mu} c_{jk}^{\nu} \tag{5}$$

n_k is the number of electrons assigned to the molecular orbital $\psi_k(\vec{r})$.

To demonstrate the quality of our SCC-Xα calculations, we compare experimental molecular ionization potentials [3] and dipole moments [4] with corresponding calculated values for SnX_2, SnX_4 (X = Cl, Br, I) and CH_3SnH_3, SnY (Y = O, S, Se, Te) presented in Tables 1 and 2. It turns out that the calculated ionization

Table 1. Comparison of experimental molecular ionization potentials (in eV) with corresponding values obtained from SCC-Xα calculations for SnX_2 and SnX_4 (X = Cl, Br, I)

	$SnCl_2$		$SnBr_2$		SnI_2	
Orbital	exp.	SCC-Xα	exp.	SCC-Xα	exp.	SCC-Xα
$2a_1$	15.81	15.95	15.56	15.60	15.50	14.91
$2b_2$	12.69	13.15	12.05	12.58	11.19	11.64
$1b_1$	12.02	12.20	11.33	11.41	10.35	10.63
$3a_1$	12.02	12.20	11.33	11.41	10.35	10.31
$1a_2$	11.27	11.70	10.58	10.96	9.55	9.91
$3b_2$	11.27	11.52	10.58	10.81	9.23	9.76
$4a_1$	10.31	10.69	9.83	10.14	9.05	9.32

	$SnCl_4$		$SnBr_4$		SnI_4	
Orbital	exp.	SCC-Xα	exp.	SCC-Xα	exp.	SCC-Xα
$2a_1$	17.00	16.57	16.70	16.12	16.10	15.52
$2t_2$	14.00	14.42	13.20	13.78	12.10	12.68
$1e$	12.71	12.63	11.75	11.84	10.29	10.66
$3t_2$	12.44	12.52	11.75	11.77	10.78	10.56
$1t_1$	12.10	12.26	11.12	11.59	10.10	10.36

Table 2. Experimental and calculated dipole moments for CH_3SnH_3 and SnY

	CH_3SnH_3	SnO	SnS	SnSe	SnTe
Experimental	0.68	4.32	3.18	2.82	2.19
Calculated	0.72	4.11	3.28	2.94	2.30

potentials deviate from the corresponding experimental values by less than 0.6 eV, and the results for other compounds (SnH_4, SnY) show the same level of agreement with experimental data. Moreover, from the good agreement between experimental and theoretical dipole moments we conclude that our calculated charge distributions are at least qualitatively correct being a necessary condition for obtaining reliable $\rho(0)$-values.

3. Isomer shift and electronic charge density at the ^{119}Sn nucleus

The experimental Mössbauer isomer shift for ^{119}Sn is given as

$$\delta = 534 \frac{\delta R}{R} [\rho_A(0) - \rho_S(0)] = \alpha \cdot \Delta\rho(0) [mms^{-1}] \tag{6}$$

where $\delta R/R$ is the fractional change in the nuclear charge radius R between the first excited state and the ground state of the ^{119}Sn nucleus. $\Delta\rho(0) = \rho_A(0) - \rho_S(0)$ is the difference between the total relativistic electronic charge densities $\rho_A(0)$

and $\rho_S(0)$ at the nucleus of the absorber and source, respectively, and α is the isomer shift calibration constant. The total electronic charge density $\rho(0)$ at the ^{119}Sn nucleus consists of valence and core contributions:

$$\rho(0) = \rho_{\text{val}}(0) + \rho_{\text{core}}(0) = \sum_k n_k |\psi_k(0)|^2 + 2 \sum_n |\psi_n^{(c)}(0)|^2. \tag{7}$$

The valence contribution $\rho_{\text{val}}(0)$ derived within the LCAO approximation arises almost entirely from the direct contribution of the tin valence electrons, i.e.

$$\rho_{\text{val}}(0) = \sum_{ij} P_{ij}^{oo} \phi_i^{(o)}(0) \phi_j^{(o)}(0) \tag{8}$$

where the atomic orbitals $\phi_i^{(o)}(0)$ and $\phi_j^{(o)}(0)$ are both on the tin atom denoted by the superscript o. The bond-order matrix elements P_{ij}^{oo} are obtained from the MO calculation.

Since the SCC-Xα method is a valence-electron-only MO-method, in calculating the core contribution $\rho_{\text{core}}(0)$ the molecular core wave functions $\psi_n^{(c)}(\vec{r})$ have to be constructed by Schmidt orthogonalization of the atomic core wave functions $\phi_n^{(c)}(\vec{r})$ to all molecular orbitals $\psi_k(\vec{r})$ [5]:

$$|\psi_n^{(c)}\rangle = N_n \left\{ 1 - \sum_k |\psi_k\rangle\langle\psi_k| - \sum_{m=1}^{n-1} |\psi_m^{(c)}\rangle\langle\psi_m^{(c)}| \right\} |\phi_n^{(c)}\rangle \tag{9}$$

Thus, the value of the nth completely orthogonalized core orbital $\psi_n^{(c)}(0)$ at the ^{119}Sn nucleus consists of three terms:

$$\psi_n^{(c)}(0) = N_n \{ \phi_n^{(c)}(0) + \delta_n^{\text{MO}}(0) + \delta_n^{\text{AO}}(0) \} \tag{10}$$

where N_n is a normalization constant. $\phi_n^{(c)}(0)$ is the free-atom core orbital, modified according to the charge state of the tin atom in the respective molecule, $\delta_n^{\text{MO}}(0)$ represents the orthogonalization of $\phi_n^{(c)}(\vec{r})$ to all MO's $\psi_k(\vec{r})$, while $\delta_n^{\text{AO}}(0)$ arises from reorthogonalizing the MO-orthogonalized core orbitals to each other [5].

The central problem of calculating $\rho(0)$ lies in the consistent combination of the atomic data for the core orbitals with the results of the valence-electron-only MO calculation. The following approximations are inherent in our calculations:

(1) The values $\phi_n^{(c)}(0)$ and $\phi_i^{(o)}(0)$ of the core and valence orbitals at the Sn nucleus are derived from relativistic atomic calculations as a function of the 5s and 5p orbital populations x_s, x_p of tin in various charge states yielding an interpolation formula of the type

$$\sqrt{4\pi}\phi(0) = a_0 + a_s x_s + a_p x_p + a_{ss} x_s^2 + a_{sp} x_s x_p + a_{pp} x_p^2 \tag{11}$$

(2) Comparative test calculations have shown that with sufficient accuracy overlap integrals between tin core wave functions and the valence orbitals of the neighbouring atoms may be computed with the HF-wave functions of Clementi and Roetti [6] for the tin atom.

(3) Electronic charge density differences $\Delta\rho(0)$ due to contributions from $p_{1/2}$ electrons are negligible (less than 0.5 a_0^{-3}).

On the basis of these approximations we are able to discuss relations and connections between the following theoretical and experimental data:

(a) the valence orbital population numbers x_s, x_p of the tin atom, (b) the effective charge Q^{Sn} of the tin atom, (c) the respective coordination number of the tin atom, (d) the various contributions to the electronic charge density $\rho(0)$ at the ^{119}Sn nucleus, namely the valence contribution, the contribution of the free tin ion corresponding to its actual charge state in the molecule, and the orthogonalization contribution, and (e) the experimental Mössbauer isomer shifts. The isomer shift data for the Sn(II) and Sn(IV) halides [7], as well as for SnO [8], are taken from rare gas matrix isolation measurements, while the isomer shift values for the other Sn compounds [9] correspond to experiments in the solid state.

From the numerical results summarized in Tables 3–5 and Fig. 1 we draw the following conclusions:

(1) The large isomer shift values for the two-coordinated Sn(II) compounds are due to the existence of a "lone-pair" MO in these compounds. "Lone-pair" MO, however, only means that this MO contains a considerable contribution from the tin atom, but not that two tin electrons are accommodated to this MO. To underline this, the character of the "lone-pair" MO, which is the highest occupied $4a_1$ molecular orbital in the Sn(II) halides SnX_2, is analysed in Table 6, where the tin 5s and 5p electron contributions, as well as the halogen valence orbital contributions are shown. These data indicate that the 5s electrons of the tin atom contribute a considerable amount to the $4a_1$ MO. It is mainly this "lone-pair" MO causing an increase in the 5s orbital population and resulting in a large electronic charge density $\rho(0)$.

(2) The small isomer shift differences between the four-, five- and six-coordinated Sn(IV) compounds are then understood due to the absence of a "lone-pair" MO in all these compounds. Therefore, calculated electronic densities are less sensitive against changes in the coordination number and simple electrostatic models are sufficient to interpret the experimental data within these series of Sn compounds [1].

(3) Within a series of equal geometrical coordination the isomer shift δ is less caused by the (indirect) influence of the 5p electrons and the electronegativity of the ligands but mainly by the difference in the (direct) 5s electron contributions. This is confirmed by theory as well as by experiment. For example, the electronic charge density $\rho(0)$ decreases, while the electronegativity of the halogen atoms increases, i.e.: $\rho(0)(SnI_m) > \rho(0)(SnF_m)$, $m = 2, 4, 6$.

Correspondingly, the experimental isomer shifts decrease in the same direction and are determined by the variation of the valence contribution to $\rho(0)$, whereas the sum of the free ion and orthogonalization terms is approximately constant (cf. Table 3).

Table 3. Effective charge Q^{Sn} and valence orbital populations x_s, x_p of the tin atom together with calculated electronic charge density contributions (in a_0^{-3}) and experimental isomer shifts δ relative to SnO_2 (in mms^{-1}) for Sn(II) compounds

Compound	Q^{Sn}	x_s	x_p	Free ion[a]	Orthogonalization	Valence	Total[a]	δ_{SnO_2}
SnI_2	0.394	1.859	1.410	47.39	−1.53	63.36	109.06	3.18
$SnBr_2$	0.554	1.812	1.268	47.43	−1.33	62.87	108.96	3.17
$SnCl_2$	0.749	1.767	1.128	48.31	−2.18	62.71	108.84	3.09
SnF_2	0.903	1.694	0.925	49.06	−2.61	61.26	107.69	2.82
$Sn_2F_5^-$	0.910	1.870	1.085	51.20	−9.41	68.23	109.98	3.31
SnTe	0.189	1.885	1.556	48.67	−2.30	62.70	109.06	3.47
SnSe	0.255	1.863	1.450	50.47	−4.24	62.47	108.68	3.35
SnS	0.374	1.857	1.326	50.92	−4.87	63.13	109.17	3.30
SnO	0.641	1.825	1.100	49.82	−3.25	63.87	110.43	2.95

[a] The values for the total electronic charge density and for its free ion contribution listed in this table are reduced by 189 900 a_0^{-3}, respectively

Table 4. Effective charge Q^{Sn} and valence orbital populations x_s, x_p of the tin atom together with calculated electronic charge density contributions (in a_0^{-3}) and experimental isomer shifts δ relative to SnO_2 (in mms^{-1}) for four-coordinated Sn(IV) compounds

Compound	Q^{Sn}	x_s	x_p	Free ion[a]	Orthogonalization	Valence	Total[a]	δ_{SnO_2}
SnI_4	0.679	0.912	1.434	46.44	7.40	32.94	86.85	1.39
$SnBr_4$	0.976	0.757	1.224	46.99	7.29	28.29	82.64	1.03
$SnCl_4$	1.329	0.609	1.023	48.46	7.47	23.72	79.74	0.75
SnF_4	1.595	0.415	0.747	48.66	6.74	16.69	72.15	−0.09
CH_3SnI_3	0.790	0.936	1.372	47.65	6.79	34.12	88.64	1.50
CH_3SnBr_3	0.988	0.779	1.210	48.36	7.28	29.12	84.85	1.41
CH_2SnCl_3	1.254	0.633	1.063	50.41	7.38	24.43	82.32	1.25
CH_3SnH_3	0.607	0.721	0.972	50.29	7.71	25.76	83.88	1.28
SnH_4	0.520	0.647	0.831	50.08	7.73	22.88	80.80	1.13

[a] The values for the total electronic charge density and for its free ion contribution listed in this table are reduced by 189 900 a_0^{-3}, respectively

Table 5. Effective charge Q^{Sn} and valence populations x_s, x_p of the tin atom together with calculated electronic charge density contributions (in a_0^{-3}) and experimental isomer shifts δ relative to SnO_2 (in mms^{-1}) for five- and six-coordinated Sn(IV) compounds

Compound	Q^{Sn}	x_s	x_p	Free ion[a]	Orthogonalization	Valence	Total[a]	δ_{SnO_2}
SnS_2 (SnS_6^{-2})	0.394	0.760	1.194	47.55	5.63	28.34	81.58	1.22
SnI_6^{2-}	0.580	0.883	1.560	45.52	5.83	31.59	82.99	1.16
$SnI_4Br_2^{2-}$	0.628	0.849	1.497	45.73	5.92	30.55	82.26	1.02
$SnI_4Cl_2^{2-}$	0.752	0.806	1.419	46.24	6.01	29.44	81.74	0.99
$SnBr_5^-$	0.867	0.764	1.313	46.36	6.47	28.26	81.14	0.97
$SnBr_4I_2^{2-}$	0.690	0.776	1.479	46.06	5.74	28.17	80.03	0.90
$SnBr_6^{2-}$	0.739	0.738	1.422	46.33	5.70	26.95	79.03	0.76
$SnCl_4I_2^{2-}$	0.919	0.689	1.319	47.06	5.93	25.67	78.74	0.67
$SnBr_4Cl_2^{2-}$	0.852	0.700	1.343	46.94	5.60	25.89	78.49	0.66
$SnCl_5^-$	1.207	0.629	1.095	47.63	6.78	24.18	78.67	0.61
$SnCl_4Br_2^{2-}$	0.960	0.658	1.264	47.45	5.67	24.64	77.82	0.57
$SnBr_4F_2^{2-}$	0.894	0.664	1.231	46.53	5.72	24.69	76.98	0.45
$SnCl_6^{2-}$	1.065	0.614	1.185	47.93	5.79	23.27	77.04	0.42
$SnCl_4F_2^{2-}$	1.100	0.576	1.071	47.72	5.65	21.96	75.38	0.29
SnO_2 (SnO_6^{2-})	1.457	0.517	0.824	47.31	6.73	20.41	74.49	0.00
SnF_6^{2-}	1.188	0.483	0.858	46.65	5.57	18.61	70.87	−0.36

[a] The values for the total electronic charge density and for its free ion contribution listed in this table are reduced by 189 900 a_0^{-3}, respectively

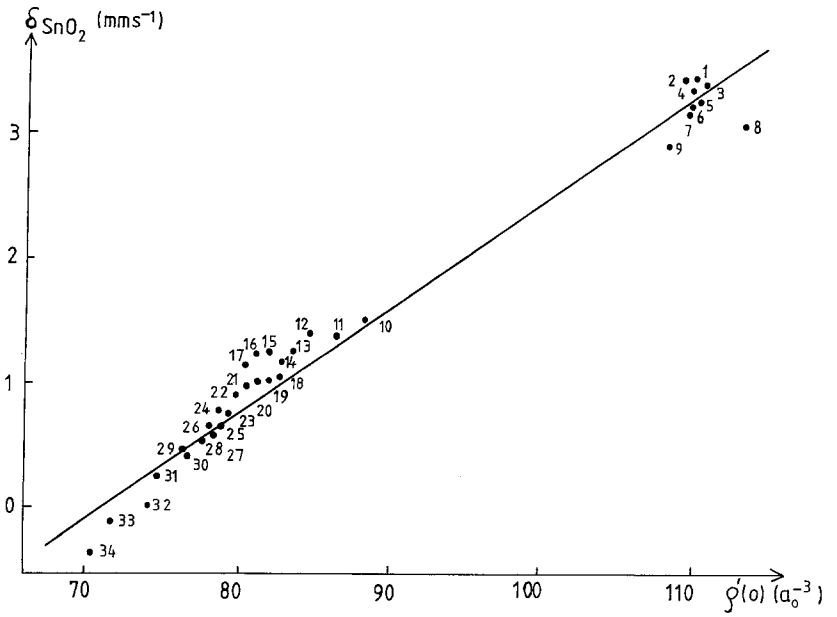

Fig. 1. Experimental isomer shifts δ relative to SnO_2 (in mms^{-1}) plotted versus calculated relativistic electronic charge densities $\rho'(0) = \rho(0) - 189\,900$ (in a_0^{-3}) at the ^{119}Sn nucleus. The various Sn compounds are numbered as follows: 1. SnTe; 2. SnSe; 3. $Sn_2F_5^-$; 4. SnS; 5. SnI_2; 6. $SnBr_2$; 7. $SnCl_2$; 8. SnO; 9. SnF_2; 10. CH_3SnI_3; 11. SnI_4; 12. CH_3SnBr_3; 13. CH_3SnH_3; 14. SnI_6^{2-}; 15. CH_3SnCl_3; 16. $SnS_2(SnS_6^{2-})$; 17. SnH_4; 18. $SnBr_4$; 19. $SnI_4Br_2^{2-}$; 20. $SnI_4Cl_2^{2-}$; 21. $SnBr_5^-$; 22. $SnBr_4I_2^{2-}$; 23. $SnCl_4$; 24. $SnBr_6^{2-}$; 25. $SnCl_4I_2^{2-}$; 26. $SnBr_4Cl_2^{2-}$; 27. $SnCl_5^-$; 28. $SnCl_4Br_2^{2-}$; 29. $SnBr_4F_2^{2-}$; 30. $SnCl_6^{2-}$; 31. $SnCl_4F_2^{2-}$; 32. $SnO_2(SnO_6^{2-})$; 33. SnF_4; 34. SnF_6^{2-}. The value of the calibration constant is $\alpha = 0.086\ mms^{-1}\ a_0^3$

Table 6. Analysis of the $4a_1$ orbital in the Sn(II) halides SnX_2

X	%-Sn(5s)	%-Sn(5p)	%-X_2
F	45	21	34
Cl	26	20	54
Br	23	21	56
I	16	17	67

(4) The large isomer shift differences between the Sn(II) compounds on the one hand and the four-, five- and six-coordinated Sn(IV) compounds on the other hand turn out to be determined by essentially two effects opposite in direction. The first enlarging effect is the above-mentioned "lone-pair" MO in Sn(II) compounds, while the second diminishing effect is a significant difference approximately up to 9 a_0^{-3} between the orthogonalization contributions for Sn(II) compounds compared with Sn(IV) compounds. Thus, these differences are non-negligible when Sn compounds of different coordination numbers are considered, i.e. the isomer shift δ and the electronic charge density $\rho(0)$ are no longer determined by the valence contribution alone. The orthogonalization of the atomic

core orbitals to the molecular orbitals prevents an overestimation of the electronic charge density differences $\Delta\rho(0)$ due to the valence contribution, leading to a considerable reduction of $\Delta\rho(0)$.

(5) In conclusion, it must be pointed out that the large isomer shift differences between the Sn(II) and Sn(IV) compounds cannot be interpreted in terms of simple model considerations based on effective atomic charges. For example, the isomer shift δ of SnF_2 is nearly three times larger than in case of $SnBr_4$, while the effective charge Q^{Sn} of the tin atom is approximately equal in both compounds.

Therefore, our results show the inadequacy in general of phenomenological schemes reviewed by Parish [10] and often used to correlate isomer shifts for Sn compounds on the basis of the 5s and 5p orbital populations of the Sn atom only.

In Fig. 1 the experimental isomer shifts δ relative to SnO_2 are plotted versus the calculated total relativistic electronic charge densities $\rho(0)$ at the ^{119}Sn nucleus. The slope of the solid line in Fig. 1 represents the isomer shift calibration constant α for which we derive the value $\alpha = 0.086\ \text{mms}^{-1}\ a_0^3$. The fractional change $\delta R/R$ in the nuclear charge radius of ^{119}Sn can be obtained from α by the relation $\alpha = 534\ \text{mms}^{-1}\ a_0^3\ \delta R/R$, yielding a value of $\delta R/R$ equal to $1.61 \cdot 10^{-4}$. In comparison with the results of other authors, our $\delta R/R$ value is between the value of $1.3 \cdot 10^{-4}$ given by de Vries et al. [11] and the value of $1.8 \cdot 10^{-4}$ derived by Rothberg et al. [12] and agrees very well with that of $(1.69 \pm 0.22) \cdot 10^{-4}$ obtained by Roggwiller et al. [13].

4. Quadrupole splitting and electric field gradient at the ^{119}Sn nucleus

The quadrupole splitting ΔE_q of ^{119}Sn with a nuclear spin of 3/2 is given by the expression

$$\Delta E_q = \tfrac{1}{2} e^2 Q V_{zz} \left(1 + \frac{\eta^2}{3}\right)^{1/2} [\text{mms}^{-1}] \tag{12}$$

where Q is the nuclear quadrupole moment of the first excited state of ^{119}Sn, and V_{zz} is the electric field gradient (EFG) in the z direction. The asymmetry parameter η is related to the diagonal EFG tensor components V_{xx}, V_{yy} and V_{zz} by

$$\eta = \frac{|V_{xx} - V_{yy}|}{V_{zz}}. \tag{13}$$

The principal axes of the EFG tensor are chosen in such a way that the diagonal components are ordered as $|V_{zz}| \geq |V_{yy}| \geq |V_{xx}|$, restricting η to values between 0 and 1.

Within the framework of a MO method taking into account explicitly only the valence electrons and treating the core electrons in terms of the point-charge approximation, the evaluation of the EFG tensor $V_{\alpha\beta}$ is based on dividing the charge density of the molecule into the positive point charges Q^{core} of the atomic

cores and the charge distribution arising from the valence electrons:

$$V_{\alpha\beta} = \sum_{\nu \neq 0} Q_\nu^{\text{core}} \hat{V}_{\alpha\beta}(\vec{R}_{\nu 0}) - e_0 \sum_{\substack{\mu\nu \\ ij}} P_{ij}^{\mu\nu} \int \phi_i^{(\mu)}(\vec{r} - \vec{R}_{\mu 0}) \hat{V}_{\alpha\beta}(\vec{r}) \phi_j^{(\nu)}(\vec{r} - \vec{R}_{\nu 0}) d^3 r \tag{14}$$

e_0 is the (positive) elementary charge, and the tensor operator components $V_{\alpha\beta}(\vec{r})$ are given as

$$\hat{V}_{\alpha\beta}(\hat{r}) = [1 - \gamma(r)] \frac{3 r_\alpha r_\beta - r^2 \delta_{\alpha\beta}}{r^5} = \frac{1 - \gamma(r)}{r^3} \sum_{M=-2}^{2} C_{\alpha\beta}^{2M} Z_{2M}(\hat{r}) \tag{15}$$

where $Z_{2M}(\hat{r})$ is a real spherical harmonic, the numbers $C_{\alpha\beta}^{2M}$ are linear combinations of Gaunt numbers and $\gamma(r)$ is the Sternheimer shielding function arising from the polarization of the core electrons of the tin atom by charges outside the core. $\gamma(r)$ can be represented with sufficient accuracy by the analytical expression [14]

$$\gamma(r) = \gamma_\infty [(e^{-a(r-b)} + 1)^{-1} - (e^{ab} + 1)^{-1}] + \sum_i d_i \, e^{-c_i (r - r_i)^2} \tag{16}$$

where a, b, d_i, c_i, r_i are determined by fitting to $\gamma(r)$ calculated by atomic coupled HF calculations [15].

With respect to the LCAO basis set, one obtains several types of integrals discussed thoroughly elsewhere [16]. Accordingly we distinguish four types of electronic contributions to the EFG tensor $V_{\alpha\beta}$:

1. Valence contribution (both wave-functions at the tin atom site) given by the one-centre integral

$$\int \phi_i^{(0)}(\vec{r}) \frac{1 - \gamma(r)}{r^3} Z_{2M}(\hat{r}) \phi_j^{(0)}(\vec{r}) d^3 r = G_{2M}(L_i L_j) \langle r^{-3} \rangle_{ij} (1 - R). \tag{17}$$

Here $G_{2M}(L_i L_j)$ is a Gaunt number, $L = (lm)$, and the quantity R depends on $\gamma(r)$ by the relation

$$R = \frac{\langle \gamma(r) r^{-3} \rangle}{\langle r^{-3} \rangle}$$

where r is the distance of the external charge from the ^{119}Sn nucleus. The expectation value $\langle r^{-3} \rangle$ is determined by atomic Dirac-Slater calculations [11] as a function of the 5s and 5p orbital populations of the tin atom.

2. Overlap contribution (one wavefunction belonging to the tin atom and the other one to one of its ligands ν): these two-centre integrals have to be evaluated exactly using Eq. (16) for $\gamma(r)$.

3. Crystal field contribution (both wavefunctions at the same ligand atom ν): in this case our test-calculations show that $\gamma(r)$ can be replaced by γ_∞. The resulting

two-centre integral

$$(1-\gamma_\infty)\int \phi_i^{(\nu)}(\vec{r})\phi_j^{(\nu)}(\vec{r})\cdot|\vec{r}+\vec{R}_{\nu 0}|^{-3}Z_{2M}(\widehat{\vec{r}+\vec{R}_{\nu 0}})d^3r \tag{19}$$

can be evaluated analytically by using a partial wave expansion of irregular spherical harmonics $r^{-l-1}Z_{lm}(\hat{r})$ [17] yielding as the leading term the isotropic crystal field contribution

$$\sum_{\nu ij} P_{ij}^{\nu\nu}(1-\gamma_\infty)R_{\nu 0}^{-3}Z_{2M}(\hat{R}_{\nu 0})\delta_{ij}=(1-\gamma_\infty)\sum_{\nu} Q_{\nu\nu}R_{\nu 0}^{-3}Z_{2M}(\hat{R}_{\nu 0}) \tag{20}$$

with $Q_{\nu\nu}=\sum_i P_{ii}^{\nu\nu}$ being the net charge of the νth atom. This result corresponds to the point-charge approximation. Higher terms of the partial wave expansion yield angular dependent terms denoted as anisotropic crystal field contributions and being considerably smaller [16].

4. Three-centre contribution (both wavefunctions at different ligand atoms). The three-centre integrals are evaluated along the same lines as the crystal field contributions, and the restriction to the point-charge approximation is justified as has been shown previously [16].

To discuss on this basis the importance of the various EFG contributions, the results of our calculations on SnF_2 are summarized in Table 7 showing the various contributions to the diagonal EFG tensor components V_{yy} and V_{zz}, respectively. It is easily seen that the EFG tensor $V_{\alpha\beta}$ at the ^{119}Sn nucleus is determined almost exclusively by the valence contribution due to the 5p electrons of the tin atom. On the other hand, the overlap contribution is relatively small and the three-centre contribution is absolutely negligible. Another important feature is the almost perfect cancellation of the isotropic crystal field contribution and the core contribution, while the anisotropic crystal field contribution is much smaller. These conclusions prove true also for the other Sn(II) halides and moreover are in good agreement with our previously obtained results for iodine-containing molecules [14].

In the next step the applicability of the Townes-Dailey approximation [18] will be investigated. For the Sn(II) halides, the EFG valence contributions V_{zz}^{val} calculated by the SCC-Xα method are compared with corresponding values V_{zz}^{TD}

Table 7. Various contributions to the EFG components V_{yy} and V_{zz} (in a_0^{-3}) for SnF_2 obtained from SCC-Xα calculations

EFG contributions	V_{yy}	V_{zz}
Valence contribution	4.118	−6.521
Overlap contribution	0.751	−0.304
Core contribution	−6.418	2.202
Isotropic crystal field contribution	6.488	−2.227
Anisotropic crystal field contribution	0.283	−0.085
Three-centre contribution	−0.001	<0.001
Sum total	5.221	−6.935

Table 8. Comparison of EFG valence contributions V_{zz}^{val} calculated by the SCC-Xα method with corresponding values V_{zz}^{TD} derived from the Townes-Dailey theory, as well as the 5p orbital populations of the tin atom for the Sn(II) halides (EFG values are given in a_0^{-3})

Compound	V_{zz}^{val}	V_{zz}^{TD}	x_{p_x}	x_{p_y}	x_{p_z}
SnI_2	−6.193	−6.698	0.431	0.153	0.826
$SnBr_2$	−6.147	−6.687	0.361	0.144	0.763
$SnCl_2$	−6.200	−6.713	0.282	0.142	0.704
SnF_2	−6.521	−7.107	0.185	0.099	0.641

$V_{zz}^{TD} = 4/5 \cdot (1-R)\langle r^{-3}\rangle_{5p} \cdot [1/2(x_{p_x}+x_{p_y})-x_{p_z}]$
$R = -0.228$ (Sternheimer factor)
$\langle r^{-3}\rangle_{5p} = 22.89 - 3.23 \cdot x_s - 2.92 \cdot x_p$

derived from the Townes-Dailey theory in Table 8. In addition, the 5p orbital populations x_{p_x}, x_{p_y}, x_{p_z} of the tin atom obtained from our MO calculations are shown. However, it must be pointed out that the Townes-Dailey approximation is only applicable if the following conditions are satisfied [14]:

1. The molecular coordinate system must be identical with the main axes system of the electric field gradient.

2. The total electric field gradient V_{zz} must be determined mainly by the valence contribution V_{zz}^{val}, i.e. $V_{zz} \approx V_{zz}^{val}$.

In our case both conditions are satisfied. Thus, our calculated V_{zz}^{val} values and the corresponding V_{zz}^{TD} values obtained from the Townes-Dailey approximation show the same trend (Table 8).

Finally, the nuclear quadrupole moment Q of the first excited state of ^{119}Sn can be derived by comparing experimental quadrupole splittings ΔE_q^{exp} with calculated electric field gradients V_{zz}. Here, only the Sn(II) halides are used while SnO has been excluded since in this case our calculated $|V_{zz}|$ is significantly too small and, on the other hand, $\rho(0)$ is correspondingly too large. This result is easily understood in the following way: the MO calculation fails to reproduce the correct s-p hybridization at the Sn atom. Namely, the 5s orbital population has to be diminished, while the $5p_z$ orbital population has to be increased, i.e.

Table 9. Comparison of experimental quadrupole splittings E_q^{exp} with theoretical values ΔE_q^{MO} and ΔE_q^{TD} (in mms^{-1}) obtained from MO calculations and the Townes-Dailey approximation, respectively, as well as the corresponding EFG values V_{zz}^{MO}, V_{zz}^{TD} (in a_0^{-3}), and the asymmetry parameters η for the Sn(II) halides

Compound	ΔE_q^{exp}	ΔE_q^{MO}	ΔE_q^{TD}	V_{zz}^{MO}	V_{zz}^{TD}	η^{MO}	η^{TD}
SnI_2	2.69	2.69	2.67	−6.396	−6.698	0.883	0.781
$SnBr_2$	2.50	2.61	2.59	−6.355	−6.687	0.776	0.639
$SnCl_2$	2.81	2.55	2.53	−6.438	−6.713	0.588	0.427
SnF_2	2.65	2.71	2.69	−6.935	−7.107	0.506	0.259

stronger s-p hybridization, resulting in a smaller $\rho(0)$ value and a larger value for $|V_{zz}|$. Using the SCC-Xα method, we obtain a value of -0.0615 b for the nuclear quadrupole moment Q, whereas the Townes-Dailey approximation yields $Q = -0.0605b$. In comparison with the results of other authors, our Q value is between the value of $-0.06b$ given by Ruby et al. [19] and the value of $-0.065b$ derived by Micklitz and Barrett [20]. For the Sn(II) halides, a comparison between the experimental quadrupole splitting data $\Delta E_q^{\exp}$ [7] and the theoretical values ΔE_q^{MO}, ΔE_q^{TD} obtained from our MO calculations and from the Townes-Dailey approximation, respectively, is presented in Table 9 together with the corresponding electric field gradients V_{zz}^{MO} and V_{zz}^{TD}, as well as the asymmetry parameters η.

5. Conclusions

In summary, it has been shown that the SCC-Xα-MO procedure proves successful in the interpretation of experimental isomer shifts and quadrupole splittings for Sn compounds with different coordination numbers. The results of our MO calculations enable us to understand in a satisfactory manner the correlation between the experimental Mössbauer parameters, the coordination number of the ^{119}Sn atom and its electronic structure, i.e. the electronic charge distribution and the electric field gradient at the ^{119}Sn nucleus, as well as the population of the tin 5s and 5p orbitals. Our MO calculations on ^{119}Sn compounds demonstrate altogether that the experimental Mössbauer data cannot be reproduced satisfactorily by simple effective charge arguments or phenomenological schemes when different coordination numbers are involved. Finally, we have derived new values for the fractional change $\delta R/R$ in the nuclear charge radius and for the nuclear quadrupole moment Q of ^{119}Sn from correlating the experimental Mössbauer parameter δ and ΔE_q with the corresponding computed electronic structure data $\rho(0)$ and V_{zz}, respectively.

Acknowledgements. Financial support of the Deutsche Forschungsgemeinschaft (grant number Na 111/3-1) is gratefully acknowledged. The authors thank K. Nagorny, A. Trautwein and R. Bläs for helpful and stimulating discussions and S. Lauer for supplying us with Sternheimer factor values obtained from coupled Hartree-Fock calculations.

References

1. Winkler W, Mehner H (1984) J Radioanal Nucl Chem 82: 151
2. Grodzicki M (1980) J Phys B13: 2683
3. Novak I, Potts AW (1984) J Electron Spectrosc 33: 1; Causley GC (1977) J Electron Spectrosc 11: 383
4. Hoeft J, Lovas FJ, Tiemann E, Törring T (1970) J Chem Phys 53: 2736
5. Trautwein A, Harris FE, Freeman AJ, Desclaux JP (1975) Phys Rev B11: 4101
6. Clementi E, Roetti C (1974) At Nucl Data Tables 14: 177
7. Schichl A, Litterst FJ, Micklitz H, Devort JP, Friedt, JM (1977) Chem Phys 20: 371
8. Bos A, Howe AT, Dale BW, Becker LW (1974) J Chem Soc Faraday Trans II 70: 440
9. Flinn PA (1978) In: Shenoy GK, Wagner FE (eds) Mössbauer isomer shifts. North Holland, Amsterdam, pp 593-615

10. Parish RV (1982) Mössbauer effect reference and data journal 5: 49
11. de Vries JLKF, Trooster JM, Ros P (1975) J Chem Phys 63: 5256
12. Rothberg GM, Guimard S, Benczer-Koller N (1970) Phys Rev B1: 136
13. Roggwiller P, Kündig W (1975) Phys Rev B11: 4179
14. Grodzicki M, Lauer S, Trautwein AX, Vera A (1981) In: Stevens J, Shenoy GK (eds) Recent chemical applications of Mössbauer spectroscopy. ACS advances in chemistry series. ACS, Washington D.C., pp 3–37
15. Lauer S, Marathe VR, Trautwein A (1979) Phys Rev A19: 1852
16. Grodzicki M (1984) Croat Chem Acta 57: 1125
17. Steinborn EO, Ruedenberg K (1973) Advan Quantum Chem 7: 1
18. Townes CH, Dailey BP (1949) J Chem Phys 17: 782
19. Ruby SL, Kalvius GM, Beard GB, Smyder RE (1967) Phys Rev 159: 239
20. Micklitz H, Barrett PH (1972) Phys Rev B5: 1704